

Supplementary Material for

MRI nanoprobe based on chemical exchange saturation transfer: Ln^{III} chelates anchored on the surface of mesoporous silica nanoparticles.

Giuseppe Ferrauto,^a Fabio Carniato,^b Lorenzo Tei,^b He Hu,^a Silvio Aime,^{*a} and
Mauro Botta^{*b}

^aDepartment of Molecular Biotechnology and Health Sciences, Molecular Imaging Center, University of Torino, Via Nizza, 52, 10126, Torino, Italy.

^bDipartimento di Scienze e Innovazione Tecnologica, Università del Piemonte Orientale "Amedeo Avogadro", Viale Teresa Michel 11, 15121 Alessandria, Italy.

Materials & Methods

All chemicals were purchased from Sigma-Aldrich Co. LLC and used without further purification. Electrospray ionization mass spectra (ESI MS) were recorded on a SQD 3100 Mass Detector (Waters), operating in positive or negative ion mode, with 1% v/v formic acid in methanol as the carrier solvent.

Synthesis of the functionalized Ln(III)-DO3A complexes

The synthesis of the ligand was carried out by modifying a procedure reported in the literature (R. T. Dean and R. W. Weber, US Patent 5053503, 1991). In detail, the ligand was prepared by alkylation of DO3A(*t*BuO)₃ with benzyl-6-bromohexanoate followed by hydrogenolysis of the benzyl ester and deprotection of the *tert*-butyl esters again with a solution of CH₂Cl₂ and trifluoroacetic acid (1:1). The Ln(III) complexes were synthesized by slowly adding to a solution of the ligand in water at pH 6.5 an equimolar amount of LnCl₃ dissolved in water, maintaining the pH at 6.5 with NaOH. The mixture was stirred overnight at room temperature; then the pH was raised to 8.5 and the mixture was stirred for 2 h. Centrifugation at 10000 rpm for 5 min at 25°C allowed the separation of Ln(OH)₃ from the solution. Finally, the solvent was removed under reduced pressure leading to the formation of the desired product as a powder. ESI-MS: m/z calcd for Gd(III)-DO3A (C₂₀H₃₃GdN₄O₈): 614.8; found: 613.3 [M⁻]; calcd for Eu(III)-DO3A (C₂₀H₃₃EuN₄O₈): 609.5; found 609.3 [M⁻]; calcd for Tm(III)-DO3A

(C₂₀H₃₃TmN₄O₈): 626.4; found 625.2 [M⁻]; calcd for Tb(III)-DO3A (C₂₀H₃₃TbN₄O₈): 616.4; found 615.2 [M⁻]. All peaks related to Ln(III) complexes show the correct isotopic distribution.

Synthesis of organo-modified mesoporous support

MCM-41 was synthesized and calcined following the procedure reported in the literature (K. Suzuki, K. Ikari, H. Imai, *J. Am. Chem. Soc.* 2004, 126, 462–463).

NH₂/MCM-41: Calcined MCM-41 (1.0 g) was firstly treated under vacuum at 250 °C for 2 h to activate the surface of the support, then the material was suspended in toluene (100 mL) under a nitrogen flow and 3-aminopropyltriethoxysilane (40 wt%) was added. The mixture was stirred at 50 °C for 20 h. The suspension was then filtered and the product was washed several times with diethyl ether to remove the unreacted silane. Finally, the sample was dried at 60°C for 2 h. It is important to limit the water adsorption to preserve the properties of the silica surface. The amount of NH₂ groups exposed on the silica surface (2.1 mmol/g) and the concentration of Si-OH functionalities before (7.7 OH per nm²) and after 3-aminopropyltriethoxysilane anchoring reaction (*ca.* 2 OH per nm²) was estimated by thermogravimetric analysis.

General procedure for the anchoring of Ln(III)-DO3A complexes on NH₂/MCM-41

NH₂/MCM-41 (70 mg) was suspended in DMF (5 mL) for 30 min. In parallel, the Ln(III) complexes (50 mg) containing a free carboxylic acid was dissolved in DMF (4 mL) and activated by adding one molar equivalent of O-(7-azabenzotriazol-1-yl)-*N,N,N',N'*-tetramethyluronium hexafluorophosphate and *N,N*-diisopropylethylamine. The solutions of the activated complexes were added to the suspension of NH₂/MCM-41 and stirred at 50°C for 24 h. The suspensions were then filtered and the solids were washed several times with H₂O to remove the unreacted complexes.

The amount of Ln(III) in the final hybrid material was measured by ICP-MS technique. The elemental analyses were performed with a Thermo Scientific (Waltham, MA, USA) X5 Series inductively coupled plasma mass spectrometer. Prior to the analysis, the samples were mineralized by dissolution in 1:1 HNO₃/HF at 100°C for 24h.

Estimation of Ln(III)-DO3A chelates loading for each MSN nanoparticle: the lanthanide loading was calculated by adapting a method reported in the literature (W. J. Rieter, J. S. Kim, K. M. L. Taylor, H. An, W. Lin, T. Tarrant, W. Lin, *Angew. Chem. Int. Ed.* 2007, 46, 3680) and by assuming a spherical shape of the particles and considering a density value of 0.8 gcm⁻³.

Characterization of materials

- HRTEM images were collected on a JEOL 3010 High Resolution Transmission Electron Microscope operating at 300 kV. Specimens were prepared by dispersing the sample by sonication in isopropanol and by depositing few drops of the suspension on carbon-coated grids.
- Infrared (IR) spectra of LnDO3A-MCM-41 and the pristine porous supports were recorded under vacuum conditions in the range 4000–400 cm^{-1} at 4 cm^{-1} resolution using a Bruker Equinox 55 spectrometer.
- N_2 physisorption measurements were carried out at 77 K in the relative pressure range from 1×10^{-6} to 1 P/P_0 by using a Quantachrome Autosorb 1MP/TCD instrument. Prior to the analysis the samples were out gassed at 373 K for 3 h (residual pressure lower than 10^{-6} torr). Apparent surface areas were determined by using the BET equation, in the relative pressure range from 0.01 to 0.1 P/P_0 . Pore volume and diameter were defined by the Barret–Joyner–Halenda (BJH) approach (applied to the desorption branch).
- Thermogravimetric analyses (TGA/DTG) of materials were performed under an oxygen flow (100 mLmin^{-1}) with a SETSYS Evolution TGADTA/DSC thermobalance, heating from 50 to 1200 $^\circ\text{C}$ at $10^\circ\text{C min}^{-1}$.
- DLS experiments were carried out by using a Zetasizer NanoZS, Malvern, UK, operating in a particle size range from 0.6 nm to 6 μm and equipped with a He-Ne laser with $\lambda=633 \text{ nm}$. The samples were dispersed in water in the presence of xanthan gum (0.1 wt%) to improve particle dispersion. Before the measurement, the suspensions were sonicated for 30 min. The particles dispersed in water tend to form large aggregates that eventually precipitate. In the solution stabilised with xanthan gum this effect is strongly limited and no precipitation is observed after days.

CEST experiments

For CEST experiments, LnDO3A-MCM-41 silica were suspended in water at the concentration of 50 mg/mL and added with Xantan gum (5 mg/mL) to stabilize the suspension. In order to dissolve the silica and avoid the aggregation, they were sonicated for 45 min, 59Hz, power 80%, 37 $^\circ\text{C}$ in a ultrasonic bath. The size of silica particles was measured by dynamic light scattering (Zetasizer NanoZS, Malvern, UK)

MRI acquisitions and image analysis

Z-spectra were acquired at 7.1 T on a Bruker Avance 300 spectrometer equipped with a microimaging probe. A frequency offset range of $\pm 150 \text{ ppm}$ was investigated. A typical RARE spin–echo sequence (RARE factor varying from 4 to 32 depending on the T_2^* of the sample) with

an echo time of 3 ms and a TR value of 5 s was used. An isotropic 64×64 acquisition matrix with a FOV of 30 mm and a slice thickness of 1 mm were used. The whole sequence was preceded by a saturation scheme consisting of a continuous rectangular wave pulse 2 s with a variable radiofrequency B_1 intensity of 12-42 μ T. The Z-spectra were interpolated by smoothing splines to identify the zero-offset on a pixel-by-pixel basis of the bulk water and, then, to assess the correct ST % value over the entire range of frequency offsets investigated. Custom-made software, compiled in the Matlab platform (Mathworks Inc., Natick, MA), was used. CEST effect is calculated by using the following formula:

$$ST\% = (1 - (M_S/M_0)) * 100$$

where M_S is the intensity of the bulk water NMR signal after the irradiation on resonance ($\Delta\omega$) of the mobile proton pool and M_0 is the intensity of the bulk water NMR signal after the irradiation at $-\Delta\omega$.

T_2 -weighted images have been acquired by using a standard T_2 -weighted RARE (Rapid Acquisition with Refocused Echoes) sequence with the following parameters (TR= 5000ms, TE= 5.5s, FOV=1cmx1cm, slice thickness = 1 mm , RARE factor= 4-32 depending on the T_2^* of the sample). T_1 values have been measured by using a Saturation Recovery Spin Echo sequence (TE= 3.8 ms, 16 variable TR ranging from 50 to 5000 ms, FOV=1cm x 1cm, slice thickness = 1 mm). T_2 values have been measured by using a MSME sequence (TR= 2000ms, 10 variable TE ranging from 11 to 500 ms, FOV=1cm x 1cm, slice thickness = 1 mm).

Characterization of LnDO3A-MCM-41 silica

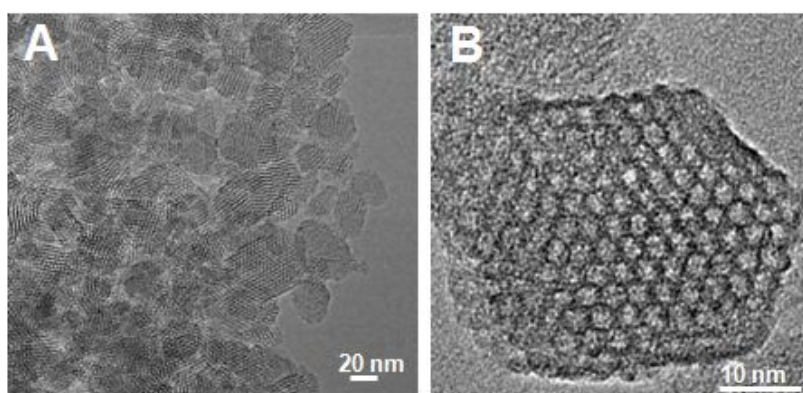


Fig. S1 HR-TEM micrographs at low (A) and high magnifications (B) of the organo-modified mesoporous silica.

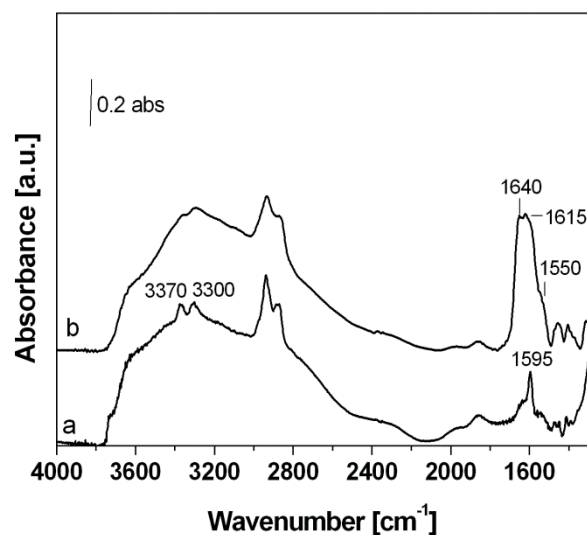


Fig. S2 IR spectra, collected at RT and under vacuum, of NH₂/MCM-41 (a) and EuDO₃A-MCM-41 degassed at room temperature.

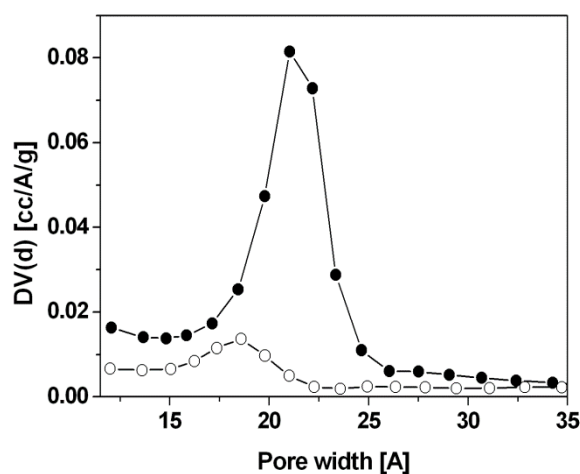


Fig. S3 Pore-diameter distribution of NH₂/MCM-41 (●) and EuDO₃A-MCM-41 (○) samples.

For all the Ln-MSNs, Z-spectra have been acquired at variable irradiation power. The results have been reported in Fig.S4-S7 for Eu-, Tm-, Tb- and GdDO₃A-MCM-41, respectively. The $B_1=24\mu\text{T}$ has been chosen for the other experiments.

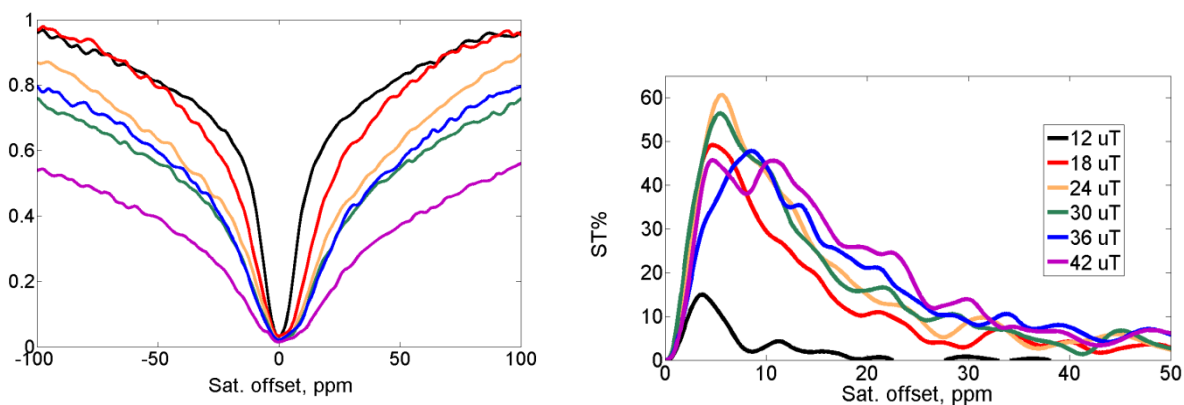


Fig. S4 Z-spectrum (left) and ST-spectrum (right) of EuDO3A-MCM-41.

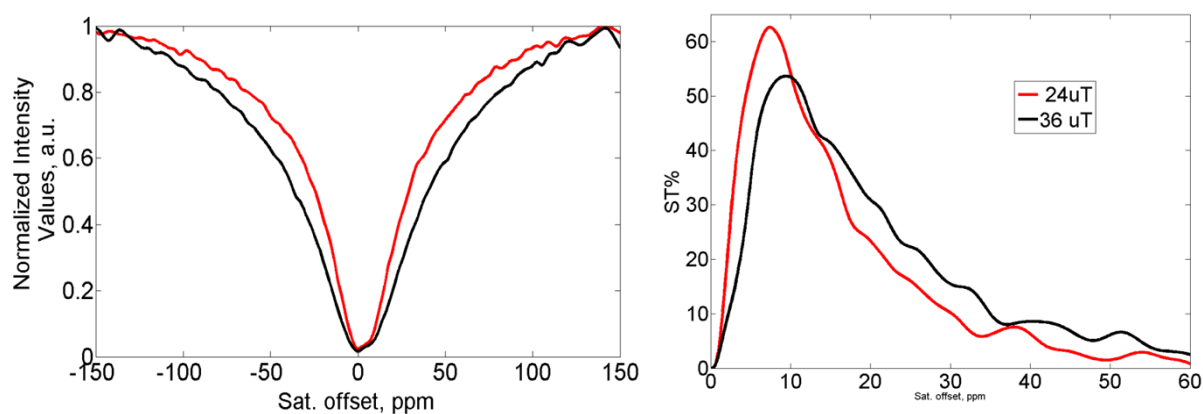


Fig. S5 Z-spectrum (left) and ST-spectrum (right) of TmDO3A-MCM-41.

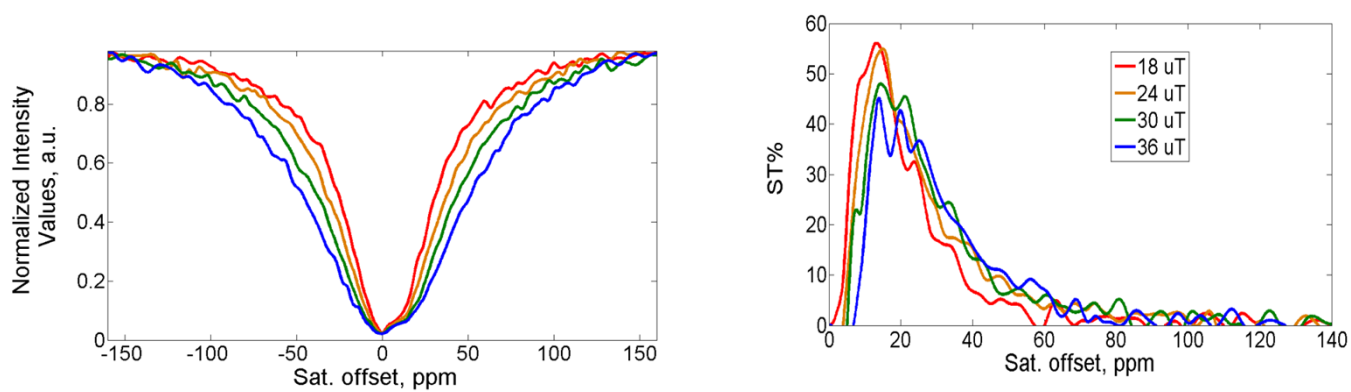


Fig. S6 Z-spectrum (left) and ST-spectrum (right) of TbDO3A-MCM-41.

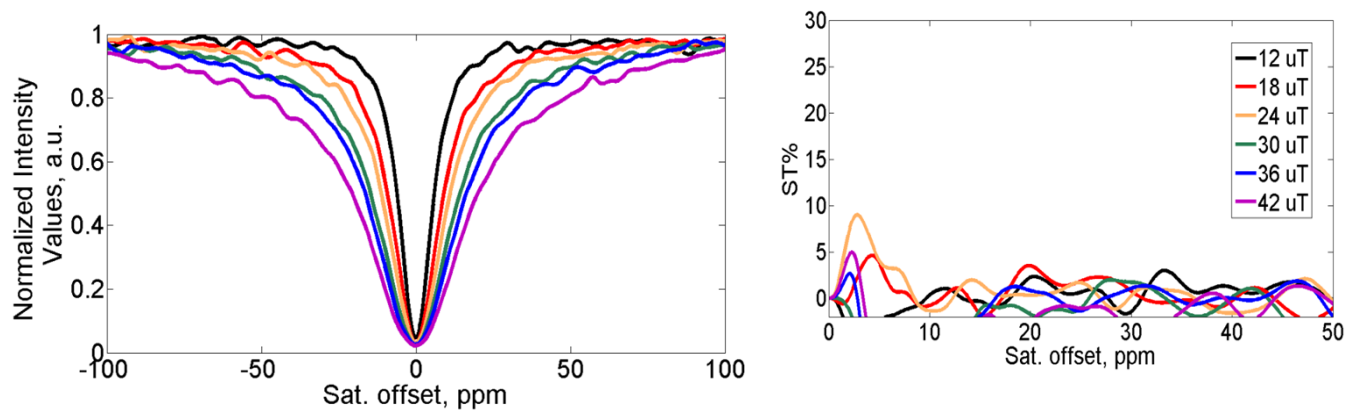


Fig. S7 Z-spectrum (left) and ST-spectrum (right) of GdDO3A-MCM-41.

The threshold for visualization of TmDO3A-MCM-41 NPs has been assessed by progressive dilution in PBS. As reported in Fig. S8, a threshold of ST% = 5% corresponds to a TmDO3A-MCM-41 concentration of ca. 2mg/mL; this value corresponds to a Tm-DO3A concentration of ca. 300 μ M .

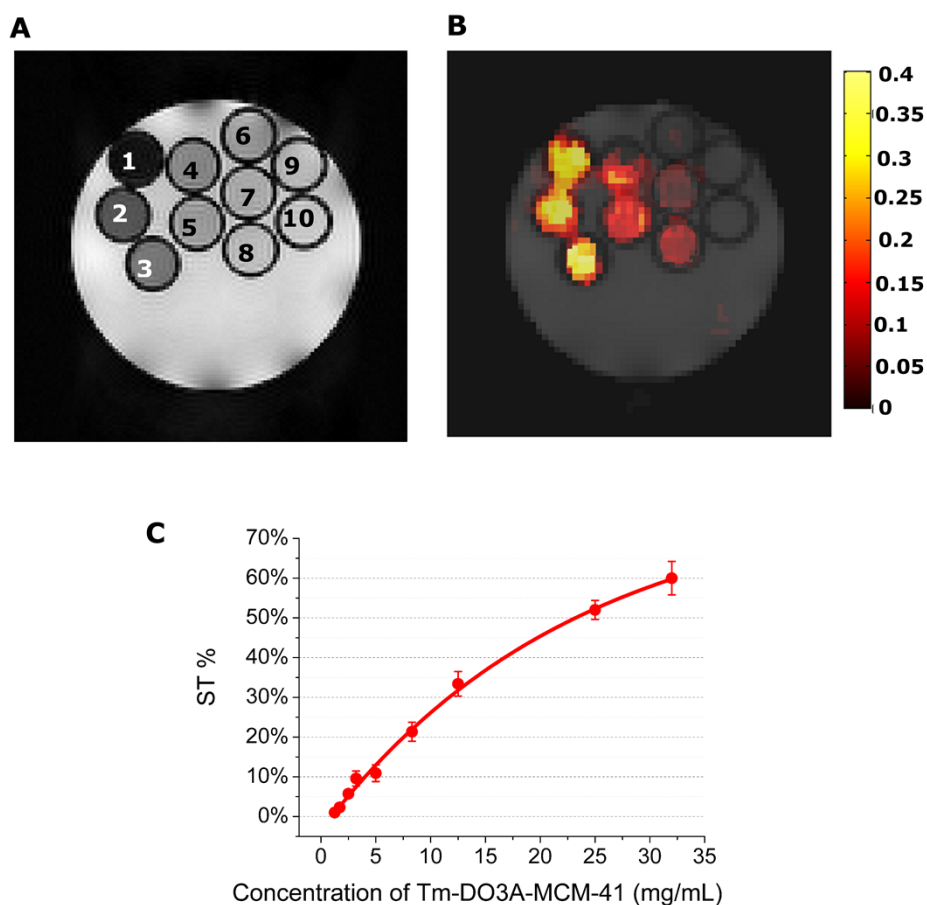


Fig. S8 T_{2w} image (A) and ST_{map} at 7.5 ppm (B) of TmDO3A-MCM-41 at variable concentration (1= 25mg/mL, 2 = 12.5mg/mL, 3 = 5mg/mL, 4 = 2.5mg/mL, 5 = 1.7mg/mL, 6 = 1.25 mg/mL, 7 = 0.83 mg/mL, 8 = 0.5mg/mL, 9 = 0.25mg/mL, 10 = 0 mg/mL); (C) ST% vs. Concentration of TmDO3A-MCM-41.

The threshold for visualization of EuDO3A-MCM-41 NPs has been assessed by progressive dilution in PBS. As reported in Fig. S9, a threshold of ST% = 5% corresponds to a EuDO3A-MCM-41 concentration of ca. 1.3mg/mL; this value corresponds to a Eu-DO3A concentration of ca. 150 μ M.

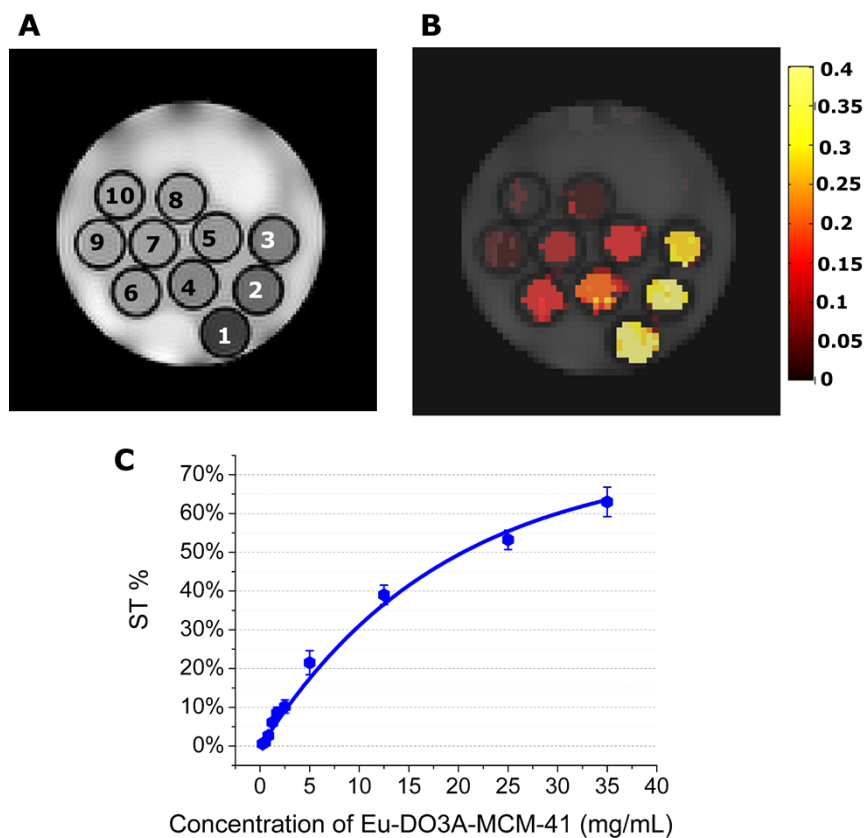


Fig. S9 T_{2w} image (A) and ST_{map} at 7.5 ppm (B) of EuDO3A-MCM-41 at variable concentration (1= 35mg/mL, 2 = 25mg/mL, 3 = 12.5mg/mL, 4 = 5mg/mL, 5 = 2.5mg/mL, 6 = 1.7mg/mL, 7 = 1.25 mg/mL, 8 = 0.83mg/mL, 9 = 0.5mg/mL, 10 = 0.25 mg/mL); (C) ST% vs. Concentration of EuDO3A-MCM-41.

pH and temperature dependence of Saturation Transfer

The pH and temperature dependences of TbDO3A-MCM-41 were also assessed to get further insight into the shift effect (Fig. S9). The ST% effect does not dramatically change in the 6-8.5 pH range. The reported pH dependence of the relaxivity of GdDO3A and GdDO3A-MCM-41 showed a substantial stability in the 4-10 pH range and a small linear decrease of r_{1p} from basic to acid pH. In the present case, the ST% effect rapidly goes down below pH 6. This behaviour could be ascribed either to an increased rate of the exchange of the pool of protons interacting with the Ln-chelates or to a substantial alteration of the silica surface and thus to a change in the interaction between the silanol groups and the LnDO3A complexes, both promoted by low pH values.

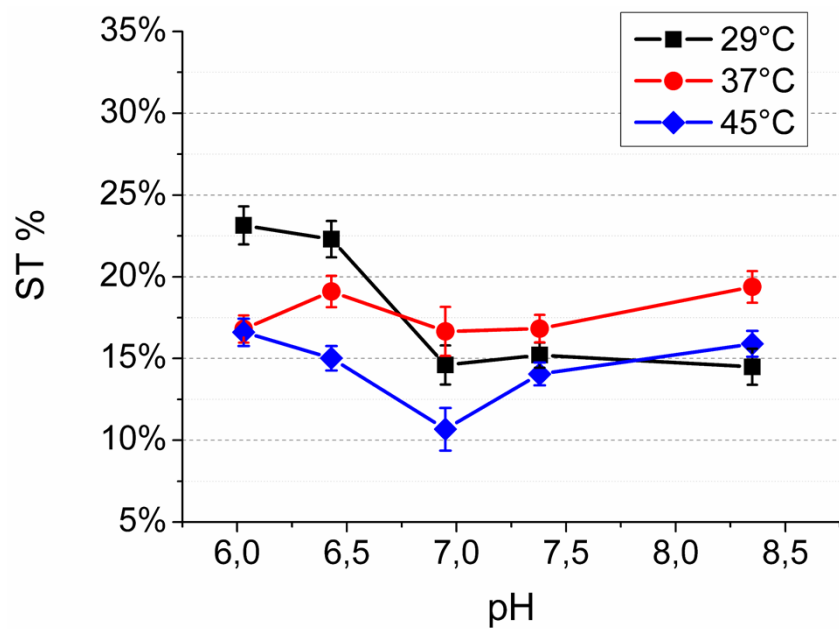


Fig. S10 ST% of TbDO3A-MCM-41 vs. pH at 29°C, 37°C and 45°C.